



Modelling the perturbation effects of the chicken litter overloading shocks on long-term semicontinuous anaerobic digesters

Modelado de los efectos de la perturbación de impulsos de sobrecarga de pollinaza sobre digestores anaeróbicos semicontinuos operados a largo plazo

G.E. Vera-Perez¹, R. Domínguez-Puerto², A. Pérez-López¹, E. Fitz-Rodríguez³, T. Espinosa-Solares^{1*}

¹Departamento de Ingeniería Agroindustrial, ²Departamento de Preparatoria Agrícola, ³Departamento de Mecánica Agrícola, Universidad Autónoma Chapingo, Carretera México-Texcoco km 38.5, Texcoco, Estado de México, C. P. 56230, México.

Received: February 1, 2023; Accepted: October 3, 2023

Abstract

Overloading shock is one of the main concerns in anaerobic digestion full-scale processes. It can lead up to digester failure. Mathematical modelling applied to biological systems allows to provide insights to the process and in that manner to propose alternatives for the overloading events. In this context, the Anaerobic Digestion Model Number 1 was implemented to simulate the digester performance during organic overloading shocks. The objective was to propose kinetic parameter values for the description and understanding of a perturbed system in order to offer alternatives for perturbed digesters. For data collection, two 10 L mesophilic anaerobic digesters were used, named A and B, working in a continuous mode and under the same operational conditions. The substrate was a 3.0 % chicken litter solution, the inoculum that came from a digester specialized in chicken litter degradation; the hydraulic retention time was 30 d. The digesters were subjected to two organic overloading pulses having a long period of time in between for digester performance recovery. Volatile fatty acids, pH, and specific methanogenic activity were used to monitor digester performance. A standard differential evolution algorithm was used for calibration; which was performed using the data of the first perturbation of digester A. Biochemical parameters related to the degradation of volatile fatty acids showed significant changes (i.e., $K_{m,c4}$ from 20.0 to 4.92 d⁻¹; $K_{m,pro}$ from 30.0 to 2.17 d⁻¹; $k_{m,ac}$ from 8.0 to 5.24 d⁻¹; $k_{m,h2}$ from 35 to 10.60 d⁻¹). After calibration, the model outputs, for digesters A and B, showed a satisfactory fit to experimental data. The result shows that differential evolution algorithm provide a robust calibration method for simulating the response of chicken litter overloading shocks in continuous methane production processes.

Keywords: disturbance, OLR, ADM1, volatile fatty acids, VFA accumulation, biogas.

Resumen

Los impulsos de sobrecarga son una de las principales preocupaciones en los procesos de digestión anaeróbica a gran escala. Puede conducir a la falla del digester. El modelado matemático aplicado a sistemas biológicos permite dar una idea del proceso y así proponer alternativas para los eventos de sobrecarga. En este contexto, se implementó el Modelo Número 1 de Digestión Anaeróbica para simular el desempeño del digester durante impulsos de sobrecarga orgánica. El objetivo fue proponer valores de parámetros cinéticos para la descripción y comprensión de un sistema perturbado con el fin de ofrecer alternativas para digestores perturbados. Para la toma de datos se utilizaron dos digestores anaeróbicos mesófilos de 10 L, denominados A y B, trabajando en modo continuo y bajo las mismas condiciones de operación. El sustrato fue una solución de 3.0 % de pollinaza, el inóculo provino de un digester especializado en la degradación de pollinaza; el tiempo de retención hidráulica fue de 30 d. Los digestores se sometieron a dos pulsos de sobrecarga orgánica con un largo período de tiempo entre ellos para recuperar el desempeño del digester. Se usaron ácidos grasos volátiles, pH y actividad metanogénica específica para monitorear el desempeño del digester. Se usó un algoritmo estándar de evolución diferencial para la calibración; que se realizó utilizando los datos de la primera perturbación del digester A. Los parámetros bioquímicos relacionados con la degradación de los ácidos grasos volátiles mostraron cambios significativos (i.e., $K_{m,c4}$ de 20.0 a 4.92 d⁻¹; $K_{m,pro}$ de 30.0 a 2.17 d⁻¹; $k_{m,ac}$ de 8.0 a 5.24 d⁻¹; $k_{m,h2}$ de 35 a 10.60 d⁻¹). Después de la calibración, los resultados del modelo, para los digestores A y B, mostraron un ajuste satisfactorio a los datos experimentales. El resultado muestra que el algoritmo de evolución diferencial proporciona un método de calibración robusto para simular la respuesta de choques de sobrecarga de pollinaza en procesos continuos de producción de metano.

Palabras clave: disturbio, velocidad de carga orgánica, ADM1, ácidos grasos volátiles, acumulación de AGV, biogás.

* Corresponding author. E-mail: tespinosas@chapingo.mx;

<https://doi.org/10.24275/rmiq/IA23168>

ISSN:1665-2738, issn-e: 2395-8472

1 Introduction

Manure management contributes to 10 % of greenhouse emissions in the livestock sector, estimated at 8.1 gigatonnes of CO₂-eq FAO (2022). In manure, nitrogen is released mainly in the form of nitrous oxide and ammonia, which contributes to public health hazards (Malomo *et al.*, 2018). Chicken litter management, having a high content of organic nitrogen, could have a critical impact on the environment (Meneses-Reyes *et al.*, 2018). This fact takes more relevance since the USDA projects a 2 percent annual demand growth through 2031 (USDA, 2022). Anaerobic digestion (AD) has had an increasing relevance in recent years as a renewable energy source utilizing organic residues (e.g., manure, food waste, and crop residues) (Scarlat *et al.*, 2018). Galvan-Arzola *et al.* (2022) reported that nitrogen inhibition of AD plays an important role in Latin America. AD is a complex multistage process performed by different groups of microorganisms in oxygen absence. These stages include hydrolysis, acidogenesis, acetogenesis, and methanogenesis. The performance of the methane process depends on the dynamic equilibrium of the microbial communities of these stages (Amin *et al.*, 2021). It is important to point out that usually AD takes place in a single digester; thus, it has several implications on defining the operational conditions for methane production.

The microorganisms involved in AD have different growing temperatures and duplication times (Amin *et al.*, 2021). These characteristics have an important influence in defining the operational conditions in full-scale processes. The common practice is defining both temperature and hydraulic retention time (HRT) for the process. In most cases, temperature is the main variable to control. Under controlled conditions of temperature, feed composition, and mass flow inlet, microorganisms can be adapted to a specific feed, and consequently, methane production can be achieved successfully (Theuerl *et al.*, 2019). However, if there is an unbalance in these operational conditions, methane production can change and even could be jeopardized (He *et al.*, 2017). The digester disturbance depends on the temporal and spatial scale, Shade *et al.* (2012) consider the press and pulse disturbances, which play an important role in the microbial community responses. These authors reported a review of the theoretical aspects of the resistance and resilience of microbial communities. Organic loading rate (OLR) disturbance can be observed when the digester input is modified by either the organic matter concentration or the flow rate. AD overloading is observed frequently in full-scale plants, Berninghaus and Radniecki (2022) indicated that depending on the amount and duration of shock loads; the digester can show resistance and

resilience, for low shock events, or from disturbance to failure, for repeated large shocks.

Mathematical modelling applied to biological systems allows to provide insights and alternatives for overcoming these hurdles. Batstone *et al.* (2002a) proposed the Anaerobic Digestion Model No. 1 (ADM1); which has been widely used for different AD processes. García-Diéguez *et al.* (2011) used the ADM1 for optimizing a control strategy based on the disturbances in the feed. Spyridonidis *et al.* (2018) applied ADM1 to simulate slaughterhouse byproducts treatment; the structure of the model was suitable for predicting the response of small or medium disturbances, but not for abrupt organic shocks. ADM1 was capable of simulating overloading shocks up to 6 times the original feed inlet (Huang *et al.*, 2018). ADM1 has been applied to define the substrate-feeding regime to satisfy specific requirements by means of solving multi-objective optimization using genetic algorithms (GA) (Ashraf *et al.*, 2022). An alternative for ADM1 is the BioModel (Gaspari *et al.*, 2022), which has been used for simulating inhibitory events caused by volatile fatty acids (VFAs).

The digester performance is highly related to the structure of the microbiome, which varies according to, among other factors, inoculum, feedstock, and operational conditions (Theuerl *et al.*, 2019). Rivas-Garcia *et al.* (2020) reported a modified ADM1 model considering the microbial composition. In fact, two identical assembled reactors, having a similar microbial structure at the beginning, under ammonia inhibition conditions might lead to differences in microbial communities (Lv *et al.*, 2019). Taking into consideration the digester performance dependence on microbiome structure, the calibration of the parameters for simulating a specific AD system is essential. In this sense, minimizing the difference between experimental and simulated results (i.e., VFAs, biogas, or methane partial pressure) has been used for calibration. This can be achieved by using straightforward or complex strategies. Wichern *et al.* (2009), simulating fermentation grass silage, observed a better fit using GA than manual calibration. For AD chicken litter process, Rivera-Salvador *et al.* (2014) reported a better simulation quality using a standard differential evolution algorithm (DEA) than the manual calibration coupled with non-linear square errors. GA was successfully used for simulating AD of organic fraction municipal solid waste at different OLRs (Fatollahi *et al.*, 2020). Modelling systems with dynamic organic loading can challenge the ADM1, which is a common situation in full-scale plants (Ozkan-Yücel & Gökçay, 2010). ADM1 has been able to simulate a full-scale anaerobic digester under variable conditions, i.e., biogas flow rate varying from practically zero to 6000 m³ d⁻¹, (Baquerizo *et al.*, 2021). In this context, the ADM1 was implemented

in the present work to simulate organic overloading shocks for parallel bioreactors under a long adaptation period to chicken litter as feedstock in order to offer alternatives for perturbed digesters. The objective was to propose kinetic parameter values, which allow a better description and understanding of a perturbed system. The experiments included two main disturbances, having in between a recovery time of 9.6 HRTs, for the digesters. The model was calibrated using one disturbance of one digester; it was challenged to simulate a second disturbance as well as a parallel digester with two disturbances.

2 Materials and methods

2.1 Experimental set-up and operation conditions

The experimental set-up has been previously described by (Meneses-Reyes *et al.*, 2018). For this experiment, two digesters (A and B), 10 L working volume and 3 L head space each in a semi-continuous mode, were fed with a target of 3 % chicken litter solution in the period considered to have a low and constant OLR, $0.653 \pm 0.104 \text{ gVS L}^{-1} \text{ d}^{-1}$. Before this perturbation experiment, the digesters were fed with the same feed for 7 HRT, i.e., 210 d using an HRT of 30 d. After this stable feed period, two overloading disturbance pulses were applied (Figure 1a), which included the increase of both concentration and volume fed. The first disturbance was between days 0 and 10, using an average OLR of $4.62 \text{ gVS L}^{-1} \text{ d}^{-1}$; while the second one was between days 301 and 311, with a OLR of $4.08 \text{ gVS L}^{-1} \text{ d}^{-1}$. Thus, the shocks were close to sevenfold and sixfold OLR, respectively. Figure 1b shows the evolution of pH and methane percentage of digesters A and B; it shows that both digesters performed in a very similar manner. In fact, when the overloading shocks were applied, the perturbation response was a reduction in methane percentage in a similar manner for both digesters.

The HRT for the no disturbance period along the experiment was 30 d. Since the flow rate increased during the disturbances, the HRT for the first and second disturbances was 20 d, which lasted for 11 d. Along the experiments, the VFAs profile, methane percentage, volatile solids (VS), and total solids (TS) were evaluated weekly, while the biogas was daily. The methodology used for collecting the analytical methods (Meneses-Reyes *et al.*, 2017) and for biogas measurements (Meneses-Reyes *et al.*, 2018) have been previously reported.

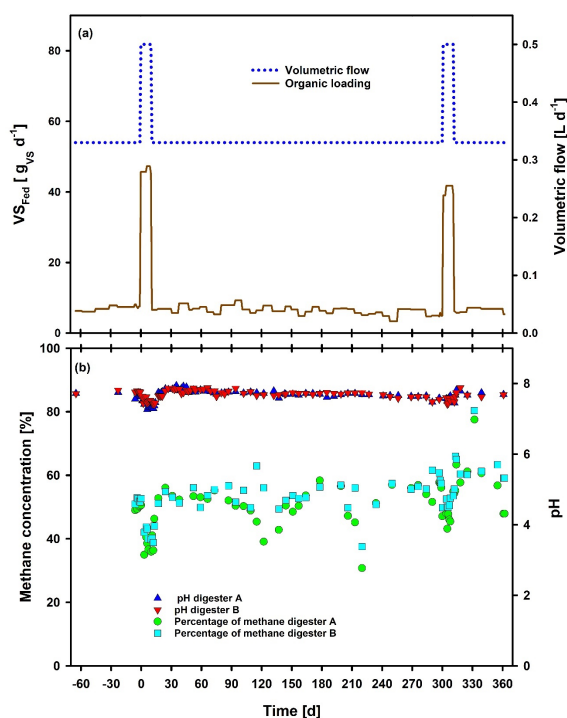


Figure 1. (a) Feeding inflow in digesters A and B. (b) Methane percentage and pH performance during experiments in digesters A and B.

Table 1. Chemical composition of chicken litter and the proportion of each component in VS and distribution of the VS degradable fraction.

Component	TS [%]	VS [%]	Degradable part VS [%]
Total volatile solids (TVS)	69.61	-	
Crude protein (CP)	37.27	53.54	51.99
Ether extract (EE)	2.73	3.92	
Crude fiber (CF)	24.52	35.22	
Free nitrogen extract (FNE)*	5.1	7.32	7.32
Ash (Fixed solids)	30.39	-	

*FNE = TVS - (CP+EE+CF)

2.2 Substrate

Chicken litter was used as a substrate in the entire experiment. Meneses-Reyes *et al.* (2017) reported the chicken litter chemical composition. Based on that information the substrate characteristics as a function of TS, and the organic components were calculated and presented in Table 1.

2.3 Model implementation

The model was implemented in MATLAB/Simulink® using the adaptation proposed by Rosen, Vrecko, Gernaey, Pons, and Jeppsson (2006), which consist of 19 biochemical process, 6 acid-based reactions, and 3 liquid-gas transfer process. The model includes 35 ordinary differential equations and 4 algebraic equations. The equations were solved by ODE 15s algorithm available in MATLAB. Equation 1 describes the dynamic state variables in the liquid phase.

$$\frac{dS_{liq,i}}{dt} = \frac{q_{in,i}S_{in,i}}{V_{liq}} - \frac{S_{liq,i}q_{out,i}}{V_{liq}} + \sum_{j=1-19} \rho_j V_{i,j} \quad (1)$$

Where $q_{in,i}$ and $q_{out,i}$, are inlet and outlet flow of digester ($L d^{-1}$); $S_{in,i}$ and $S_{liq,i}$ are the concentration ($kg_{COD} m^{-3} \cdot g_{COD} L^{-1}$) of composite i in the influent stream and liquid phase, respectively. V_{liq} is the reactor working volume (L), the term $\sum_{j=1-19} \rho_j V_{i,j}$ is the sum of the products between kinetic rates ρ_j and stoichiometric factors $V_{i,j}$. The interaction liquid gas transfer is described by Equation 2.

$$\rho_{i,T} = k_{L,i}(S_{liq,i} - K_{H,i}P_{i,gas}) \quad (2)$$

Where $\rho_{i,T}$ is an additional rate term, $k_{L,i}$ is the overall mass transfer coefficient (d^{-1}), $K_{H,i}$ is the equilibrium constant from Henry's law to the gas i ($M bar^{-1}$). $P_{i,gas}$ is the partial pressure of gas i (bar) (Batstone *et al.*, 2002a).

Initial dynamic state variables were taken from (Rosén & Jeppsson, 2006). Excluding organics composites concentration in the liquid phase and hydrogen, carbon dioxide, and methane concentration in the gas phase were set at 0 at the beginning of the process.

2.4 Model input matrix

The degradable fraction of substrate is a key factor for defining organic compounds that enter to the process, and it influences the model performance, in the present work, the degradable fraction was taken as the degradable VS (DVS) since VS correspond to the degradable fraction. The degradable fraction of substrate was 59.31 %, which was estimated based on biochemical methane potential study reported by our research group (Meneses-Reyes *et al.*, 2017). It can be noted, in Table 1, that the major component of organic matter considered degradable was the protein; this criterion was based on the predominance of microorganisms related to protein degradation in food waste during and after press disturbance (He *et al.*, 2017). Li, He, Yan, Chen, and Dai (2017) showed the dominance of metabolic and transport of amino acids in high solids dewatered sludge systems. It has been reported that the conversion of protein was the most relevant metabolic pathway in acid and alkali

primary sludge fermentation (Huang *et al.*, 2018). Additionally, lipids and crude fiber were taken as a non-degradable fraction of the organic matter. Lipids had a negligible concentration; additionally, it has been reported that lipids present a low water solubility that could form micelles, which makes difficult the degradation (Labatut, 2012). Since, crude fiber is composed mainly of recalcitrant composites (Usman Khan & Ahring, 2021), its degradation was considered negligible. All free nitrogen extract was taken as degradable. In the case of protein, the value was adjusted to the estimated DVS.

The amount of each composite in the model input $S_{in,i}$ was obtained by Equation 3.

$$S_{in,i} = \frac{S_T X_i}{q_{in}} COD_{th,i} \quad (3)$$

Where S_T is the total organic matter (g_{vs}), fed daily X_i is the mass fraction of each composite (i.e., carbohydrates, proteins, and lipids) concerning the total. $COD_{th,i}$ is the theoretical conversion factor ($g_{COD} g^{-1} VS$) that varies according to the composite and can be obtained by Equation 4 (Koch, Lübken, Gehring, Wichern, & Horn, 2010).

$$COD_{th,i} = \frac{16[2a + 0.5(b - 3d) - c]}{12.0107a + 1.00784b + 15.999c + 14.0067d} \quad (4)$$

Where a , b , c , and d are the numbers of carbon, hydrogen, oxygen, and nitrogen, respectively. The organic nitrogen in the input to the model was taken from experimental ammoniacal nitrogen in the substrate (Batstone *et al.*, 2002a); which was fitted as a function of TS to estimate daily ammoniacal nitrogen.

2.5 Parameters calibration

The calibration was performed using a standard DEA as reported by (Rivera-Salvador *et al.*, 2014). The parameters of the algorithm were set as follows: crossover probability = 0.2; differential variation factor = 0.9; population size = 60, and accuracy = 10^{-6} . 28 parameters of ADM1 were calibrated that involve the process, as follows: disintegration and hydrolysis first order kinetic uptake rates (K_{dis} , $K_{hyd,ch}$, $K_{hyd,pr}$, $K_{hyd,li}$), Monod maximum uptake specific rate for acidogenesis, acetogenesis, and methanogenesis ($K_{m,su}$, $k_{m,aa}$, $k_{m,fa}$, $K_{m,c4}$, $K_{m,pro}$, $k_{m,ac}$, $k_{m,h2}$), Monod half saturation constants ($K_{S,su}$, $K_{S,aa}$, $K_{S,fa}$, $K_{S,c4}$, $K_{S,ac}$, $K_{S,h2}$, $K_{S,pro}$), yields of biomass on substrate (Y_{su} , Y_{aa} , Y_{fa} , Y_{c4} , Y_{pro} , Y_{ac} , Y_{h2}), and inhibition constants ($K_{Ih2,c4}$, $K_{Ih2,pro}$, $K_{I,nh3}$).

VFA in the previous time first disturbance (from day -65 to 0 d) and the disturbance period from bioreactor A (from day 0 to 102 d) were used for parameter calibration by fitting experimental and simulated data. The experimental period comprising

from (103 to 365 d) of the same digester (A), and entirely experimental data from digester B (-65 to 365 d), were used to validate the model. The cost function used to fit the data, in the evaluation period, has the form presented in Equation 5.

$$f(p) = \sum_{j=1-4} (\hat{y}_{ij} - y_{ij})^2 \quad (5)$$

Where f is the objective function that depends on the vector parameter p , \hat{y}_{ij} is the value in the position i^{th} by the j^{th} VFA obtained from the simulation. Meanwhile, y_{ij} is the correspondingly observed value. DEA was run ten times with 500 generations each time; the value for each parameter was reported as the average of ten replicates and its corresponding standard deviation. Simulation quality was evaluated according to Equations 6, 7, 8, and 9 (Wallach, 2006), which respectively correspond to relative root mean squared error (RRMSE), modelling efficiency (EF), agreement index (index), and correlation coefficient (r).

$$RRMSE = \frac{RMSE}{\underline{y}} \quad (6)$$

$$EF = 1 - \frac{\sum_{i=1}^N (y_i - \hat{y}_i)^2}{\sum_{i=1}^N (y_i - \underline{y})^2} \quad (7)$$

$$index = 1 - \frac{\sum_{i=1}^N (y_i - \hat{y}_i)^2}{\sum_{i=1}^N (|y_i - \underline{y}| + |\hat{y}_i - \underline{y}|)^2} \quad (8)$$

$$r = \frac{\sum_{i=1}^N [(y_i - \underline{y})(\hat{y}_i - \underline{y})]}{\sqrt{\sum_{i=1}^N [(y_i - \underline{y})^2] \sum_{i=1}^N [(\hat{y}_i - \underline{y})^2]}} \quad (9)$$

Where RMSE is the root mean square error, \underline{y} is the average of data observed, y_i is the i^{th} experimental observed value, \hat{y}_i is the i^{th} value obtained by the simulation and \underline{y} is the average of simulation data.

3 Results and discussion

3.1 Digesters' performance during disturbance experiments

Two digesters were used for the experiments (A and B). As it was described in the previous section, both digesters had a similar performance, at daily bases, in terms of pH and methane percentage. The first disturbance, applied to digesters A and B, lasted for 11 d with sevenfold OLR, while the second one also lasted for 11 days with sixfold OLR. The changes in the specific methanogenic activity (SMA) and the VFA were registered throughout the entire experiment. Table 2 shows the average and range of SMA, as well as the average TVFA, before the disturbance and the maximum value register after

disturbance, which is known as resistance (Shade *et al.*, 2012) of the microbial community to the organic shock. It is important to point out, that the first disturbance produced a perturbation that needed around 2 HRT to recover for digesters A and B; while in the second disturbance, in both digesters, had a lower influence on TVFA accumulation and a shorter recovery time, around 1.5 HRT. These facts suggest the digesters experienced a kind of adaptation to the organic shock; Berninghaus and Radniecki (2022), working with stepwise overloading shocks, reported that the system had shorter recovery times as the overloading shock increases in the range of 2.5 to 9.0 gVS L⁻¹ d⁻¹. It could be attributed to the effect on methanogenic archaea populations are jeopardized since their duplication time is usually longer than the one of the fermenters (Amin *et al.*, 2021). Sun, Ni, Angelidaki, Dong, and Wu (2019), working with pig manure and glucose, have reported that when overloading take place from 6 to 9 gVS L⁻¹ d⁻¹ methane quality reduces from 65.0 to 28.0 %.

As a response to both disturbances, for digesters A and B, the perturbation of the digesters showed a decrease in SMA at the beginning of the organic shocks, which remained low during the time that the overloading shock was applied; as soon as the overload was released SMA was recovered, showing even a peak above the previous average SMA.

After disturbance, VFA concentration increased up to a peak in both digesters. The maximum concentrations, for digesters A and B expressed as gCOD L⁻¹, registered for the first perturbation are, respectively, as follows: acetate (8.7) (5.6), propionate (6.6) (4.6), butyrate (3.1) (2.2), and valerate (2.4) (2.3). For the second perturbation, the trend was quite similar but with lower concentrations. The values for digesters A and B are, respectively, as follows: acetate (4.5) (5.2), propionate (3.1) (3.5), butyrate (1.6) (1.8), and valerate (1.6) (1.6). It is important to notice that during the overloading pulse, the pH reduces slightly even the VFA peaks registered, it can be attributed to the high NH₄⁺ concentrations in chicken litter, which can have a buffer effect due to, either NH₃/NH₄⁺ or NH₃/CO₃²⁻/VFAs (Meng *et al.*, 2018). This trend has been reported for chicken manure disturbed digesters, in a semicontinuous digester subject to sudden changes with the adaptation period (Bi *et al.*, 2019) and to step-loading shocks (Wang *et al.*, 2019). In the case of food residuals, the same trend has been also observed (He *et al.*, 2017).

3.2 Model calibration

For model calibration, the beginning of the disturbance was taken as time zero. Thus, the VFA data of digester A from day -65 to 102 were used for calibration; that range of time included: (1) a stable process before

disturbance, (2) the disturbance and the following perturbation, and (3) a recovery process. Table 3 shows the parameters calibrated along with those reported in the literature. Some of the literature data reported in both tables were obtained under pulse, or press disturbance experiments for instance Batstone, Pind, and Angelidaki (2003) worked with VFA pulse disturbance using cattle manure as feedstock, while

Kalfas, Skiadas, Gavala, Stamatelatou, and Lyberatos (2006) working also with pulse VFA disturbance and soluble part of feedstock that was raw olive pulp. Koutrouli *et al.* (2009) performed the first pulse VFA disturbance followed by a press stepwise with olive pulp. Fatolah *et al.* (2020) calibrated the ADM1 by applying step loading with the organic fraction of municipal solid waste (OFMSW).

Table 2. VFAs perturbation response to disturbance in digesters.

Digester or reference	Characteristics of the experiments	Digester performance							
		State	TVFA [mg L ⁻¹]	Acetate [mg L ⁻¹]	Propionate [mg L ⁻¹]	Butyrate [mg L ⁻¹] iso-butyrate [mg L ⁻¹]	Valerate [mg L ⁻¹] iso-valerate [mg L ⁻¹]	pH	Methane production [mL CH ₄ g ⁻¹ VS] Percentage in biogas [%]
Digester A	The period from -65 to 102 d (first pulse) Scale: laboratory 10 L WV Type of disturbance: pulse OLR: 0.653 - 4.62 gVS L ⁻¹ d ⁻¹ HRT: 30-20 d	1	812.1 ± 498.4	± 636.0 ± 434.0	± 58.4 ± 37.2	23.2 ± 8.2 39.4 ± 21.6	18.0 ± 0.8 37.2 ± 18.3	7.7 ± 0.1	173.6 ± 54.7 50.0 ± 0.7
		2	15195.5	8161.7	4361.1	1088.0 608.7	369.1 820.4	7.3	37.4-495.2 35.0
	The period from 103 to 362 d (second pulse) Scale: laboratory 10 L WV Type of disturbance: pulse OLR: 0.653 - 4.08 gVS L ⁻¹ d ⁻¹ HRT: 30-20 d	1	554.4 ± 341.6	± 327.3 ± 220.4	± 78.8 ± 58.9	60.3 ± 32.5 38.9 ± 18.8	53.2 ± 27.6 50.7 ± 22.4	7.7 ± 0.1	217.2 ± 93.3 50.5 ± 6.8
		2	7837.7	4204.4	2060.4	485.6 377.5	189.0 590.8	7.5	115.6 - 849.4 43.1
	The period from -65 to 102 d (first pulse) Scale: laboratory 10 L WV Type of disturbance: pulse OLR: 0.653 - 4.62 gVS L ⁻¹ d ⁻¹ HRT: 30-20 d	1	222.8 ± 86.5	± 154 ± 67.4	± 21.8 ± 9.1	13.6 ± 1.0 13.0 ± 21.8	17.4 ± 0.2 16.2 ± 1.1	7.8 ± 0.1	195.7 ± 18.0 52.1 ± 0.7
		2	10011.6	5233.4	3048.0	720.8 505.1	359.3 778.0	7.4	35.5 - 461.3 38.8
Digester B	The period from 103 to 362 (second pulse) Scale: laboratory 10 L WV Type of disturbance: pulse OLR: 0.653 - 4.08 gVS L ⁻¹ d ⁻¹ HRT: 30-20 d	1	507.2 ± 333.6	± 266.8 ± 187.9	± 94.9 ± 71.7	54.4 ± 41.6 41.4 ± 17.0	48.5 ± 34.5 53.9 ± 23.9	7.7 ± 0.1	237.6 ± 109.7 54.3 ± 5.3
		2	8620.5	4885.2	2296.0	558.2 411.9	191.9 577.0	7.4	142.1 - 1254.0 50.0

Bi et al. (2019)	Scale: laboratory 12 L WV Type of disturbance: sudden changes with the adaptation period OLR: 1.6 - 2.5 gVS L ⁻¹ d ⁻¹ HRT: 20 d	1	340 ± 100	120 ± 70	90 ± 40	30 ± 30 20 ± 20	20 ± 20 20 ± 20	8.25	252 ± 8 68 ± 1
F. Wang et al. (2019)	Scale: laboratory 6 L WV Type of disturbance: step-loading OLR: 3.5 ± 0.1 - 15 ± 0.1 gVS L ⁻¹ d ⁻¹ HRT: 30 d	1	~ 100	~ 50	~ 20	~ 30 -	- -	6.6 ± 0.2	440 1200* ~ 60
He et al. (2017)	Scale: laboratory 30 L WV Type of disturbance: step-loading OLR: 3 - 6 gVS L ⁻¹ d ⁻¹ HRT: 23 - 46 d	1	2210 ± 180	2100 2590	-	300 - 520	- -	~ 7.5	520 59 - 64.24
	Regimen: CSTR, mesophilic Mode and substrate: semicontinuous, chicken manure	2	3010 ± 420	1550 ± 470	290 ± 110	180 ± 20 130 ± 30	140 ± 20 210 ± 80	8.27	245 ± 9 67 ± 2
	Regimen: CSTR, mesophilic Mode and substrate: semicontinuous, chicken manure	2	1412	894.9	~ 155.1	~ 77.7 ~ 206.8	~ 38.7 ~ 38.7	7.6 ± 0.2	410* ~ 30
	Regimen: CSTR, mesophilic Mode and substrate: semicontinuous, food waste	2	9443	5690	2760	~ 290 ~ 70	~ 250 ~ 450	~ 7.0	Failure Recovery phase: ~ 900 ~ 70

WV: Working volume CSTR: Continuous stirred tank reactor 1: Stable 2: Perturbation *[mL CH₄ g⁻¹V_S]

Table 3. Values of kinetic parameters in disturbances systems from literature compared to calibrated ones in the present work.

Parameter / source	K _{dis} [d ⁻¹]	K _{sp,del} [d ⁻¹]	K _{sp,pr} [d ⁻¹]	K _{sp,li} [d ⁻¹]	K _{m,ss} [d ⁻¹]	K _{S,ss} [kgCOD m ⁻³]	Y _{ss}	k _{m,ss} [d ⁻¹]	K _{S,ss} [kgCOD m ⁻³]	Y _{ss}	k _{m,fa} [d ⁻¹]	K _{S,fa} [kgCOD m ⁻³]	Y _{fa}	K _{m,e4} [d ⁻¹]	
Reference value	0.50c	10b	10b	10c	30b	0.50b	0.10a	50b	0.30a	0.08a	6c	0.40c	0.06a	20b	
Batstone et al. (2002b)															
Batstone et al. (2003)														12.0 ± 0.40 13.7	
Lübken et al. (2007)		0.31	0.31	0.31											
Wichern et al. (2009)	0.26														
Koch et al. (2010)		0.14		0.14										5	
Ozkan-Yucel and Gökçay (2010)		1	1	1	35	0.5									
Normak et al. (2015)					11.9	4.5		19.8	0.3					12.2	
Jurado, Antonopoulou, Lyberatos, Gavala, and Skiadas (2016)			3.0 × 10 ⁻³	2.8 × 10 ⁻⁴							0.93		13.1		
Fatollahi et al. (2020)					6									13.95	
Wang et al. (2022)	1.2	10	10	10	4	0.1		4	0.1		1	0.04		2	
Present work Average ¹ ± standard deviation	1.99 ± 4.03 × 10 ⁻⁸	19.99 ± 1.90 × 10 ⁻⁷	20	39.03 ± 3.46	59.87 ± 0.02	0.01 ± 1.41 × 10 ⁻⁹	0.07	100	0.21	0.06	0.01	1.58 ± 7.01 × 10 ⁻⁴	0.07 ± 1.63 × 10 ⁻⁴	4.92 ± 0.01	
Parameter / source	K _{S,e4} [kgCOD m ⁻³]	Y _{e4}	K _{sp,e4} [kgCOD m ⁻³]	k _{m,pro} [d ⁻¹]	K _{S,pro} [kgCOD m ⁻³]	Y _{pro}	K _{sp,pro} [kgCOD m ⁻³]	k _{m,ac} [d ⁻¹]	K _{S,ac} [kgCOD m ⁻³]	Y _{ac}	k _{m,i2} [d ⁻¹]	K _{S,i2} [kgCOD m ⁻³]	Y _{i2}	K _{sp,i3} [m ⁻³]	[kmol
Reference value	0.20c	0.06a	1 10 ⁻⁵ a	13b	0.10b	0.04a	3.50 10 ⁻⁶ a	8b	0.15b	0.05a	35b	7 10 ⁻⁶ b	0.06a	1.80 10 ⁻³ a	
Batstone et al. (2002b)															
Batstone et al. (2003)	0.29 ± 0.02														
Kalfas et al. (2006)				3.50 ± 0.32	0.06 ± 0.03			9.99 ± 1.2	0.31 ± 0.09						
Lübken et al. (2007)	0.357			5.5	0.392			7.1				3 10 ⁻⁵			
Koutrouli et al. (2009)				2.02 ± 0.07	0.03 ± 0.01			8.34 ± 1.02	0.96 ± 0.21						
Wichern et al. (2009)			5.4 × 10 ⁻⁸	13			4.8 10 ⁻⁸					4.2 10 ⁻⁵		8.4 10 ⁻³	
Koch et al. (2010)			5 × 10 ⁻⁸				4.6 10 ⁻⁸	4.4				5.6 10 ⁻⁵			
Ozkan-Yucel and Gökçay (2010)				2.2				10	0.18				0.05		
Normak et al. (2015)	0.6			3.5	0.4			11.1	0.5					0.0223	
Jurado et al. (2016)				6.56				45.02							
Fatollahi et al. (2020)					0.14				0.05		7.79 10 ⁻⁶				
Wang et al. (2022)	0.01			0.039	0.005			4	0.015		1.5	7 × 10 ⁻⁶			
Present work Average ¹ ± standard deviation	0.64 ± 1.03 × 10 ⁻³	0.04 ± 5.50 × 10 ⁻³⁵	1.30 10 ⁻⁵ ± 3.28 × 10 ⁻⁴²	2.17 ± 4.73 × 10 ⁻³	0.20 ± 8.80 × 10 ⁻³⁴	0.05 ± 9.83 × 10 ⁻⁷	2.45 10 ⁻⁶	5.24 ± 7.56 × 10 ⁻⁵	0.3	0.06 ± 1.65 × 10 ⁻⁸	10.60 ± 0.30	1.39 10 ⁻⁰⁵ ± 4.39 × 10 ⁻¹⁴	0.08	2.34 × 10 ⁻³	

a Varies within factor of 30% by Batstone et al. (2002b) b Varies within factor of 100 % by Batstone et al. (2002b) c Varies within factor of 300% by Batstone et al. (2002b) 1 Average of ten replicants

Eighteen kinetic, three inhibitory, and seven yield parameters were calibrated to describe the disturbance and perturbation processes comprehensively. For calibration, parameter k_{dis} , was considered for the disintegration process. Also, it was considered just the composite of organic material (e.g., proteins,

carbohydrates, and lipids) as input to the model based on the literature (Batstone et al., 2015).

DEA has shown its simplicity of use and robustness for estimating many parameters in dynamic crop models, especially DE/ran/1/bin (Trejo-Zúñiga et al., 2014). In ADM1, it was applied for calibrating

25 parameters; the simulation results showed a satisfactory fit to experimental data (Rivera-Salvador *et al.*, 2014). Despite the advantage of using DEA for estimating model parameters, it is important to define the proper boundaries to obtain reasonable values related to the process. In the present work, the space of search for each parameter was defined according to the variation proposed in the original ADM1 Batstone *et al.* (2002b).

3.2.1 Parameters of disintegration, hydrolysis and acidogenesis

The K_{dis} , $K_{hyd,ch}$, $K_{hyd,pr}$, and $K_{hyd,li}$ parameters are related to enzymatic reactions in the pool, as well as, the $K_{m,su}$ and $k_{m,aa}$ to the rate of fermentation of sugars and amino acids. As it can be seen in Table 3, these values were between one to three times larger than those reported in the literature. Fatty acids' uptake rate, $k_{m,fa}$, took the lower limit in the algorithm set-up. $K_{S,su}$, $K_{S,aa}$, and $K_{S,fa}$, the half-saturation constant for sugars, amino acids, and long-chain fatty acids, took values of 98, 30, 295 % compared to the reference. Y_{su} , Y_{aa} , and Y_{fa} are the yield parameters in sugars, amino acids, and fatty acids uptake; the first two showed a decrease of 30 %; conversely, the last showed an increase of 19 %.

3.2.2 Parameters related to acetogenesis and methanogenesis

Acetogenesis comprises the uptake of propionate and c4 (ADM1 considers that butyrate and valerate are lumped (Batstone *et al.*, 2003). For propionate, the calibrated $K_{m,pro}$, $K_{S,pro}$, and Y_{pro} parameters were smaller or slightly (28%) larger than the reference values. It can be seen in Table 3 that the uptake rate is in accordance with the obtained by Koutrouli *et al.* (2009) and Ozkan-Yücel and Gökçay (2010). The $K_{S,pro}$ showed similarity with what was reported in the literature by pulses of VFA (Koutrouli *et al.*, 2009), by stepwise overloading (Fatolahi *et al.*, 2020), and by a dynamic full-scale plant (Lübken *et al.*, 2007). $K_{m,c4}$ and Y_{c4} were smaller than the reference values. In the case of $K_{S,c4}$, the calibrated value was around two times larger than the reported value. The $K_{m,c4}$ in this work is in accordance with the reported by Ozkan-Yücel and Gökçay (2010). It is important to stress that in the case of the half-saturation constant, Normak *et al.* (2015) reported a similar value to the one obtained in this work.

For acetoclastic and hydrogenotrophic methanogens, the parameters are as follows: $k_{m,ac}$, $K_{S,ac}$, Y_{ac} , and $k_{m,h2}$, $K_{S,h2}$, and Y_{h2} , respectively. The reduction of acetate uptake rate is in agreement with Koch *et al.* (2010). These authors showed an accumulation of acetate after the TS increased in the system. For the $K_{S,ac}$ Kalfas *et al.* (2006) reported a

similar value for VFAs pulses. Uptake rate and half saturation constant values for the hydrogenotrophic pathway, showed reduction; meanwhile, the calibrated yield value increased. Inhibition parameters ($K_{Ih2,c4}$, $K_{Ih2,pro}$, and $K_{I,nh3}$) varied by a factor of 30 % concerning reference; all are in accordance with the literature.

Figures 2 and 3 show the results of the calibration process. As it can be seen, the calibrated model has a better fit to the experimental value than the model with the reference values.

3.3 Model evaluation

The calibrated parameters were evaluated in the period from 103 to 362 to digester A. The entire recorded data from digester B was also used for that purpose. Figures 2 and 4 show the outputs of the model compared with experimental data in terms of TVFA (acetate + propionate + butyrate + valerate), pH, and SMA. During the first pulse and the period for recovery, TVFA is represented more satisfactorily by the calibrated parameters than the parameters suggested by Batstone *et al.* (2002b).

A slight overestimation appears in data collected from digester B. Conversely, experimental response in the second pulse was overestimated by calibrated parameters. Both sets of parameters, referenced, and calibrated, underestimated pH but followed the same trend as data collected in both digesters. The outputs of the model overestimated the SMA during the first pulse and the period for recovery in both digesters. Conversely, SMA has underestimated the sharp increase after the second pulse in both digesters.

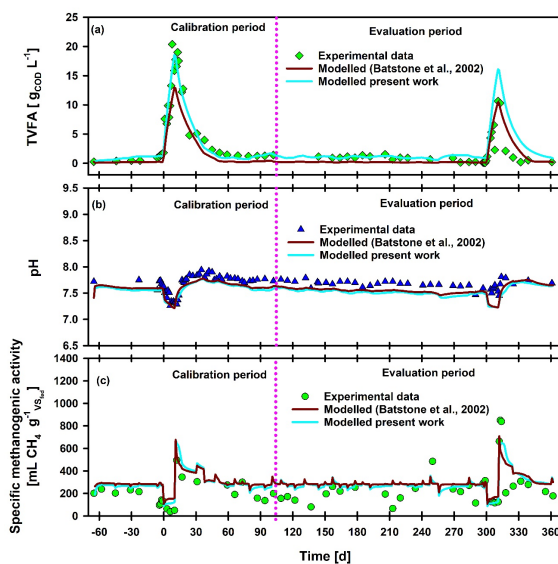


Figure 2. Comparison between experimental and simulated results of TVFA, pH, and specific methanogenic activity (SMA) in digester A.

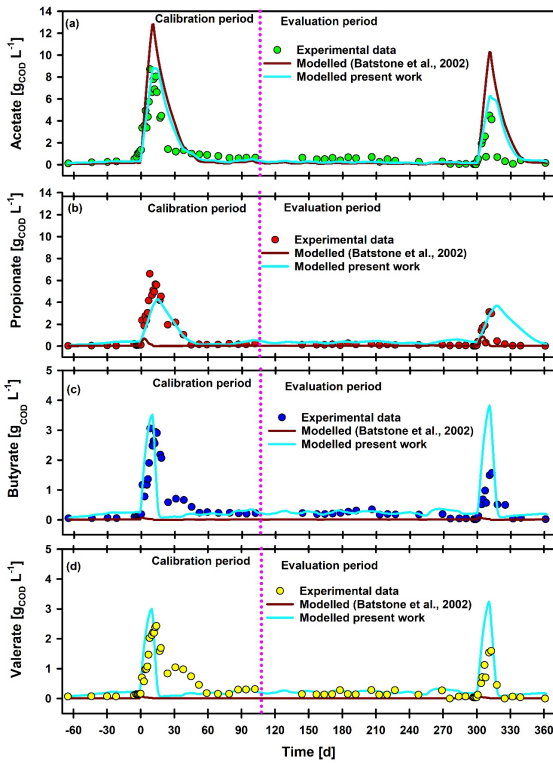


Figure 3. Comparison between experimental and simulated data of individual volatile fatty acids in digester A.

Figures 3 and 5 show the performance of individual volatile fatty acids; remarkably, the model output with parameters calibrated was better than the parameters suggested by Batstone *et al.* (2002b). Nevertheless, overestimation occurred in the second pulse to both digesters A and B.

The model fit quality is shown in Tables 4 and 5. The RRMSE can be visualized as an error related to all data measured mean. In this context, digester A, that error was diminished by the calibration. In the case of digester B, acetate, propionate, and SMA showed a decrease; butyrate, valerate, and TVFA showed an increase in this quality parameter. In both digesters, the pH did not change the trend.

The modelling efficiency parameter shows how the model is better at predicting rather than the average of experimental measurements (Wallach, 2006). The calibrated parameters improve the model prediction to digester A, except in cases of valerate and pH. For predicting acetate, propionate, and SMA of digester B, the calibrated model was better than the model that uses reference values. Another helpful parameter is the agreement index (index). For digester A, all the parameters that describe digester performance were improving with calibrated parameters except pH. To digester B, just TVFA and pH were not improved by calibrated parameters. In the case of the correlation coefficient, both digesters show the same trends; just the pH and SMA show a decrease in the positive linear correlation.

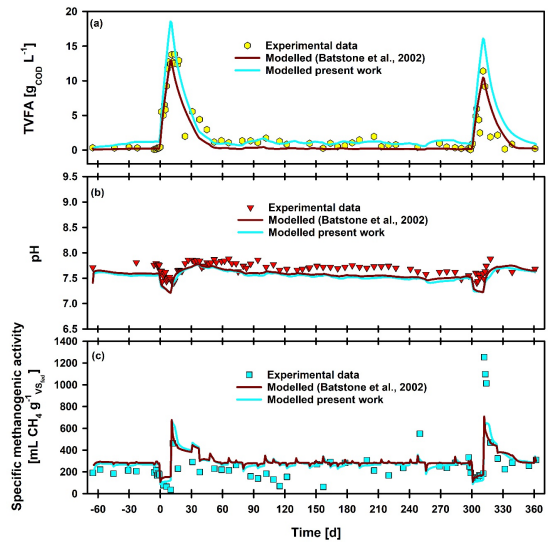


Figure 4. Comparison between experimental and simulated data of TVFA, pH, and SMA in digester B.

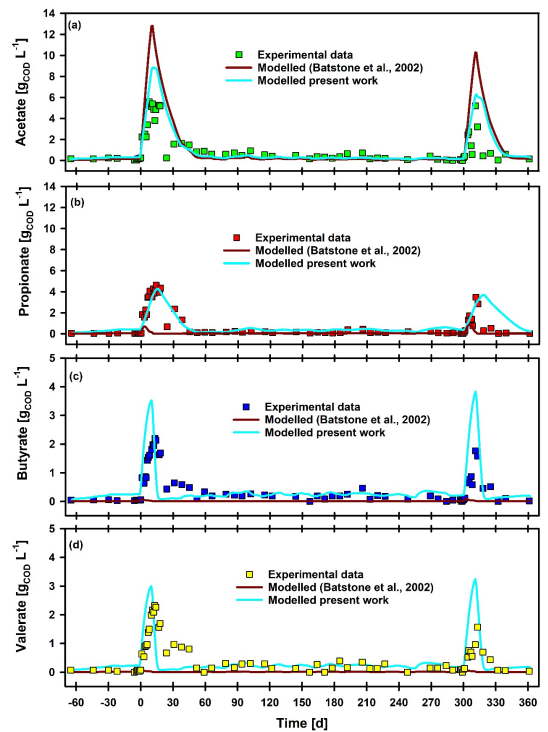


Figure 5. Comparison between experimental and simulated data of individual volatile fatty acids in digester B.

It is important to stress out that even TVFA was predicted satisfactorily by parameters suggested by Batstone *et al.* (2002b), the model did not describe the behavior of the individual VFA. The quality of the modelling for acetate, propionate and SMA was improved by calibrating parameters to both digesters. In the case of methane production, a similar conclusion is depicted by Fatollahi *et al.* (2020), when stepwise disturbances were used, and for pulse shocks (Koutrouli *et al.*, 2009).

Table 4. Evaluation of simulation quality for digester A.

Goodness-of-fit parameter	Acetate		Propionate		Butyrate		Valerate		TVFA		pH		Methane production	
	1	2	1	2	1	2	1	2	1	2	1	2	1	2
RRMSE	1.4	0.74	1.72	0.83	2.26	1.88	1.52	1.24	0.6	0.59	0.02	0.02	0.52	0.5
EF	-0.22	0.66	-0.32	0.69	-0.56	-0.09	-0.69	-0.12	0.79	0.8	-0.09	-0.43	0.44	0.49
Index	0.85	0.93	0.44	0.89	0.43	0.78	0.44	0.78	0.93	0.95	0.77	0.73	0.82	0.85
r	0.91	0.9	0.2	0.84	0.09	0.67	0.06	0.68	0.93	0.91	0.81	0.81	0.83	0.82

1: Modelled with standard parameters (Batstone *et al.*, 2002b) 1: Modelled with calibrated parameters (present work).

Table 5. Evaluation of simulation quality for digester B using calibrated parameters from digester A.

Goodness-of-fit parameter	Acetate		Propionate		Butyrate		Valerate		TVFA		pH		Methane production	
	1	2	1	2	1	2	1	2	1	2	1	2	1	2
RRMSE	2.21	1.24	1.64	0.78	1.5	1.52	1.55	1.57	0.48	0.83	0.02	0.02	0.59	0.57
EF	-2.04	0.05	-0.34	0.7	-0.72	-0.77	-0.65	-0.69	0.85	0.57	-0.81	-1.32	0.53	0.55
Index	0.74	0.86	0.45	0.91	0.45	0.73	0.43	0.73	0.96	0.92	0.71	0.66	0.78	0.81
r	0.9	0.9	0.22	0.85	0.08	0.66	0.02	0.66	0.93	0.92	0.77	0.78	0.82	0.78

1: Modelled with standard parameters (Batstone *et al.*, 2002b) 1: Modelled with calibrated parameters (present work).

In the case of c4, the accumulation during disturbance was overestimated. Conversely, when low dynamic OLR was applied, the model predicted very satisfactorily, as seen in Figures 3 and 5 for the VFAs mentioned above.

Conclusions

$K_{m,c4}$, $K_{m,pro}$, $k_{m,ac}$, and $k_{m,h2}$ showed the most significant changes during calibration. The model outputs, for digesters A and B, showed a better fit with experimental data regarding modelling efficiency (EF) and the indexes of the modelling (index) than the original ADM1 parameters. The result shows that DEAs provide a robust calibration method for simulating the response of chicken litter overloading shocks in continuous methane production processes. The calibration performed to the ADM1, along with the validation, allowed to predict the experimental data; thus, in the case of a disturbance, it has the advantage for taking control actions before perturbation takes place. The next challenges are to evaluate the predictive capacity of the model and to define its implementation in the operation of the digester in real-time.

Acknowledgment

The present work was funded by the Dirección General de Investigación y Posgrado, Universidad Autónoma Chapingo, through the project 23141-C-62 entitled “Monitoreo y estabilización de biodigestores alimentados con diferentes sustratos para obtener microbiomas resistentes a condiciones de perturbación capaces de incrementar la producción

de metano en el biogás”. The authors would like to thank to the Consejo Nacional de Humanidades, Ciencias y Tecnologías (CONAHCYT) (México) for the scholarship (Number 774595) granted to Gerson Esteban Vera-Pérez. Furthermore, express their gratitude to Dr. Christian Rosen and to Dr. Ulf Jeppsson for providing the initial MATLAB implementation of ADM1.

Nomenclature

OLR	Organic Loading Rate ($\text{gVS L}^{-1}\text{d}^{-1}$)
HRT	Hydraulic Retention Time (d)
q	Flow (L d^{-1})
i	Component index
S_i	Concentration of soluble component i (nominally gCOD L^{-1})
X_i	Concentration of insoluble or particulate component i (nominally gCOD L^{-1})
V	Volume (L)
in, out	Inlet or outlet stream
liq	Liquid phase of reactor
gas	Gas phase of reactor
Y_i	Yield of biomass on substrate (gCOD_X , gCOD_S^{-1} or dimensionless)
ρ_j	rate for process j (gCOD L^{-1})
T	Temperature (K)
t	time (d)
k_{La}	gas-liquid transfer coefficient (d^{-1})
$K_{H,i}$	equilibrium constant from Henry's law to the gas i , (M bar^{-1})
P_i	Partial pressure of gas i , (bar)
K_{dis}, K_{hyd}	First-order disintegration or hydrolysis rate (d^{-1})
$K_{S,i}$	Monod half saturation constant (gCOD L^{-1})

$K_{m,i}$	Specific Monod maximum uptake rate ($\text{g}_{COD} \text{L}^{-1}, \text{S} \cdot \text{g}_{COD} \text{L}^{-1}, \text{X} \text{d}^{-1}$ or d^{-1})
K_I	Inhibition constant (nominally $\text{g}_{COD} \text{L}^{-1}$)
ch, pr, li	Carbohydrates, proteins, or lipids
su, aa, fa	Monosaccharides, amino acids, or fatty acids
$c4, pro, ac, h2$	Valerate and butyrate, propionate, acetate, and hydrogen
$nh3$	ammonium

References

- Amin, F. R., Khalid, H., El-Mashad, H. M., Chen, C., Liu, G., & Zhang, R. (2021). Functions of bacteria and archaea participating in the bioconversion of organic waste for methane production. *Science of the Total Environment* 763. doi: [10.1016/j.scitotenv.2020.143007](https://doi.org/10.1016/j.scitotenv.2020.143007)
- Ashraf, R. J., Nixon, J. D., & Brusey, J. (2022). Using multi-objective optimisation with ADM1 and measured data to improve the performance of an existing anaerobic digestion system. *Chemosphere* 301. doi: [10.1016/j.chemosphere.2022.134523](https://doi.org/10.1016/j.chemosphere.2022.134523)
- Baquerizo, G., Fiat, J., Buffiere, P., Girault, R., & Gillot, S. (2021). Modelling the dynamic long-term performance of a full-scale digester treating sludge from an urban WRRF using an extended version of ADM1. *Chemical Engineering Journal* 423. doi: [10.1016/j.cej.2021.128870](https://doi.org/10.1016/j.cej.2021.128870)
- Batstone, D. J., Keller, J., Angelidaki, I., Kalyuzhnyi, S. V., Pavlostathis, S. G., Rozzi, A., . . . Vavilin, V. A. (2002a). The IWA Anaerobic Digestion Model No 1 (ADM1). *Water Science and Technology : A journal of the International Association on Water Pollution Research* 45(10), 65-73. doi: [10.2166/wst.2002.0292](https://doi.org/10.2166/wst.2002.0292)
- Batstone, D. J., Keller, J., Angelidaki, I., Kalyuzhnyi, S. V., Pavlostathis, S. G., Rozzi, A., . . . Vavilin, V. A. (2002b). *Anaerobic Digestion Model No. 1 (ADM1), IWA task group for mathematical modelling of anaerobic digestion processes*. IWA Publishing.
- Batstone, D. J., Pind, P. F., & Angelidaki, I. (2003). Kinetics of thermophilic, anaerobic oxidation of straight and branched chain butyrate and valerate. *Biotechnology and Bioengineering* 84(2), 195-204. doi: [10.1002/bit.10753](https://doi.org/10.1002/bit.10753)
- Batstone, D. J., Puyol, D., Flores-Alsina, X., & Rodríguez, J. (2015). Mathematical modelling of anaerobic digestion processes: applications and future needs. *Reviews in Environmental Science and Biotechnology* 14(4), 595-613. doi: [10.1007/s11157-015-9376-4](https://doi.org/10.1007/s11157-015-9376-4)
- Berninghaus, A. E., & Radniecki, T. S. (2022). Shock loads change the resistance, resiliency, and productivity of anaerobic co-digestion of municipal sludge and fats, oils, and greases. *Journal of Cleaner Production* 362. doi: [10.1016/j.jclepro.2022.132447](https://doi.org/10.1016/j.jclepro.2022.132447)
- Bi, S., Qiao, W., Xiong, L., Ricci, M., Adani, F., & Dong, R. (2019). Effects of organic loading rate on anaerobic digestion of chicken manure under mesophilic and thermophilic conditions. *Renewable Energy* 139, 242-250. doi: doi.org/10.1016/j.renene.2019.02.083
- FAO. (2022). GLEAM 2.0 - Assessment of greenhouse gas emissions and mitigation potential. Retrieved from <https://www.fao.org/gleam/results/en/>
- Fatolahi, Arab, G., & Razaviarani, V. (2020). Calibration of the Anaerobic Digestion Model No. 1 for anaerobic digestion of organic fraction of municipal solid waste under mesophilic condition. *Biomass and Bioenergy* 139. doi: [10.1016/j.biombioe.2020.105661](https://doi.org/10.1016/j.biombioe.2020.105661)
- Galvan-Arzola, U., Miramontes-Martinez, L. R., Escamilla-Alvarado, C., Botello-Alvarez, J. E., Alcalá-Rodríguez, M. M., Valencia-Vázquez, R., & Rivas-García, P. (2022). Anaerobic digestion of agro-industrial waste: Anaerobic lagoons in Latin America. *Revista Mexicana de Ingeniería Química* 21(2). doi: [10.24275/rmiq/IA2680](https://doi.org/10.24275/rmiq/IA2680)
- García-Diéguez, C., Molina, F., & Roca, E. (2011). Multi-objective cascade controller for an anaerobic digester. *Process Biochemistry* 46(4), 900-909. doi: [10.1016/j.procbio.2010.12.015](https://doi.org/10.1016/j.procbio.2010.12.015)
- Gaspari, M., Alvarado-Morales, M., Tsapekos, P., Angelidaki, I., & Kougias, P. (2022). Simulating the performance of biogas reactors co-digesting ammonia and/or fatty acid rich substrates. *Biochemical Engineering Journal*, 108741. doi: doi.org/10.1016/j.bej.2022.108741
- He, Q., Li, L., & Peng, X. (2017). Early warning indicators and microbial mechanisms for process failure due to organic overloading in food waste digesters. *Journal of Environmental Engineering* 143(12). doi: [10.1061/\(asce\)ee.1943-7870.0001280](https://doi.org/10.1061/(asce)ee.1943-7870.0001280)

- Huang, Dong, W., Wang, H., & Feng, Y. (2018). Role of acid/alkali-treatment in primary sludge anaerobic fermentation: Insights into microbial community structure, functional shifts and metabolic output by high-throughput sequencing. *Bioresource Technology* 249, 943-952. doi: doi.org/10.1016/j.biortech.2017.10.104
- Jurado, E., Antonopoulou, G., Lyberatos, G., Gavala, H. N., & Skiadas, I. V. (2016). Continuous anaerobic digestion of swine manure: ADM1-based modelling and effect of addition of swine manure fibers pretreated with aqueous ammonia soaking. *Applied Energy* 172, 190-198. doi: [10.1016/j.apenergy.2016.03.072](https://doi.org/10.1016/j.apenergy.2016.03.072)
- Kalfas, H., Skiadas, I. V., Gavala, H. N., Stamatelatos, K., & Lyberatos, G. (2006) Application of ADM1 for the simulation of anaerobic digestion of olive pulp under mesophilic and thermophilic conditions. *Water Science and Technology* 54, 149-156.
- Koch, K., Lübken, M., Gehring, T., Wichern, M., & Horn, H. (2010). Biogas from grass silage - Measurements and modeling with ADM1. *Bioresource Technology* 101(21), 8158-8165. doi: [10.1016/j.biortech.2010.06.009](https://doi.org/10.1016/j.biortech.2010.06.009)
- Koutrouli, E. C., Kalfas, H., Gavala, H. N., Skiadas, I. V., Stamatelatos, K., & Lyberatos, G. (2009). Hydrogen and methane production through two-stage mesophilic anaerobic digestion of olive pulp. *Bioresource Technology* 100(15), 3718-3723. doi: [10.1016/j.biortech.2009.01.037](https://doi.org/10.1016/j.biortech.2009.01.037)
- Labatut, R. A. (2012). Anaerobic biodegradability of complex substrates: performance and stability at mesophilic and thermophilic conditions. PhD Thesis, Cornell University. <https://hdl.handle.net/1813/29168>
- Li, N., He, J., Yan, H., Chen, S., & Dai, X. (2017). Pathways in bacterial and archaeal communities dictated by ammonium stress in a high solid anaerobic digester with dewatered sludge. *Bioresource Technology* 241, 95-102. doi: [10.1016/j.biortech.2017.05.094](https://doi.org/10.1016/j.biortech.2017.05.094)
- Lübken, M., Wichern, M., Letsiou, I., Kehl, O., Bischof, F., & Horn, H. (2007) Thermophilic anaerobic digestion in compact systems: Investigations by modern microbiological techniques and mathematical simulation. *Water Science and Technology* 56, 19-28.
- Lv, Z., Leite, A. F., Harms, H., Glaser, K., Liebetrau, J., Kleinstaub, S., & Nikolausz, M. (2019). Microbial community shifts in biogas reactors upon complete or partial ammonia inhibition. *Applied Microbiology and Biotechnology* 103(1), 519-533. doi: [10.1007/s00253-018-9444-0](https://doi.org/10.1007/s00253-018-9444-0)
- Malomo, G. A., Bolu, S. A., Madugu, A. S., & Usman, Z. S. (2018). Nitrogen emissions and mitigation strategies in chicken production. *Animal Husbandry and Nutrition*. InTech.
- Meneses-Reyes, Hernández-Eugenio, G., Huber, D. H., Balagurusamy, N., & Espinosa-Solares, T. (2017). Biochemical methane potential of oil-extracted microalgae and glycerol in co-digestion with chicken litter. *Bioresource Technology* 224, 373-379. doi: [10.1016/j.biortech.2016.11.012](https://doi.org/10.1016/j.biortech.2016.11.012)
- Meneses-Reyes, J. C., Hernández-Eugenio, G., Huber, D. H., Balagurusamy, N., & Espinosa-Solares, T. (2018). Oil-extracted *Chlorella vulgaris* biomass and glycerol bioconversion to methane via continuous anaerobic co-digestion with chicken litter. *Renewable Energy* 128, 223-229. doi: [10.1016/j.renene.2018.05.053](https://doi.org/10.1016/j.renene.2018.05.053)
- Meng, X., Yu, D., Wei, Y., Zhang, Y., Zhang, Q., Wang, Z., ..., Wang, Y. (2018). Endogenous ternary pH buffer system with ammonia-carbonates-VFAs in high solid anaerobic digestion of swine manure: An alternative for alleviating ammonia inhibition? *Process Biochemistry* 69, 144-152. doi: doi.org/10.1016/j.procbio.2018.03.015
- Normak, A., Suurpere, J., Suitso, I., Jõgi, E., Kokin, E., & Pitk, P. (2015). Improving ADM1 model to simulate anaerobic digestion start-up within inhibition phase based on cattle slurry. *Biomass and Bioenergy* 80, 260-266. doi: [10.1016/j.biombioe.2015.05.021](https://doi.org/10.1016/j.biombioe.2015.05.021)
- Ozkan-Yucel, U. G., & Gökçay, C. F. (2010). Application of ADM1 model to a full-scale anaerobic digester under dynamic organic loading conditions. *Environmental Technology* 31(6), 633-640. doi: [10.1080/09593331003596528](https://doi.org/10.1080/09593331003596528)
- Rivas-Garcia, P., Botello-Alvarez, J. E., Miramontes-Martinez, L. R., Cano-Gomez, J. J., & Rico-Martinez, R. (2020). New model of hydrolysis in the anaerobic co-digestion of bovine manure with vegetable waste: Modification of anaerobic digestion, model no. 1. *Revista Mexicana de Ingeniería Química* 19(1), 109-122. doi: [10.24275/rmiq/Bio557](https://doi.org/10.24275/rmiq/Bio557)
- Rivera-Salvador, V., López-Cruz, I. L., Espinosa-Solares, T., Aranda-Barradas, J. S., Huber,

- D. H., Sharma, D., & Toledo, J. U. (2014). Application of an anaerobic digestion model No. 1 to describe the syntrophic acetate oxidation of poultry litter in thermophilic anaerobic digestion. *Bioresource Technology* 167, 495-502. doi: [10.1016/j.biortech.2014.06.008](https://doi.org/10.1016/j.biortech.2014.06.008)
- Rosén, C., & Jeppsson, U. (2006). Aspects on ADM1 Implementation within the BSM2 Framework. Retrieved from <http://www.iea.lth.se/publications/Reports/LTH-IEA-7224.pdf>
- Rosen, C., Vrecko, D., Gernaey, K. V., Pons, M. N., & Jeppsson, U. (2006) Implementing ADM1 for plant-wide benchmark simulations in Matlab/Simulink. *Water Science and Technology* 54, 11-19.
- Scarlat, N., Dallemand, J. F., & Fahl, F. (2018). Biogas: Developments and perspectives in Europe. *Renewable Energy* 129, 457-472. doi: [10.1016/j.renene.2018.03.006](https://doi.org/10.1016/j.renene.2018.03.006)
- Shade, A., Peter, H., Allison, S. D., Baho, D. L., Berga, M., Bürgmann, H., . . . Gilbert, J. (2012). Fundamentals of microbial community resistance and resilience [Review]. *Frontiers in Microbiology* 3. doi: [10.3389/fmicb.2012.00417](https://doi.org/10.3389/fmicb.2012.00417)
- Spyridonidis, A., Skamagkis, T., Lambropoulos, L., & Stamatelatos, K. (2018). Modeling of anaerobic digestion of slaughterhouse wastes after thermal treatment using ADM1. *Journal of Environmental Management* 224, 49-57. doi: [10.1016/j.jenvman.2018.07.001](https://doi.org/10.1016/j.jenvman.2018.07.001)
- Sun, H., Ni, P., Angelidaki, I., Dong, R., & Wu, S. (2019). Exploring stability indicators for efficient monitoring of anaerobic digestion of pig manure under perturbations. *Waste Management* 91, 139-146. doi: [10.1016/j.wasman.2019.05.008](https://doi.org/10.1016/j.wasman.2019.05.008)
- Theuerl, Klang, J., & Prochnow, A. (2019). Process disturbances in agricultural biogas production-causes, mechanisms and effects on the biogas microbiome: A review. *Energies* 12(3). doi: [10.3390/en12030365](https://doi.org/10.3390/en12030365)
- Trejo-Zúñiga, C. E., López-Cruz, I. L., & García-Ruiz, A. (2014). Parameter estimation for crop growth model using evolutionary and bio-inspired algorithms. *Applied Soft Computing* 23, 474-482. doi: <https://doi.org/10.1016/j.asoc.2014.06.023>
- USDA. (2022). Poultry expected to continue leading global meat imports as demand rises. Retrieved from <https://t.ly/LAnDq>
- Usman Khan, M., & Ahring, B. K. (2021). Improving the biogas yield of manure: Effect of pretreatment on anaerobic digestion of the recalcitrant fraction of manure. *Bioresource Technology* 321, 124427-124427. doi: [10.1016/j.biortech.2020.124427](https://doi.org/10.1016/j.biortech.2020.124427)
- Wallach, D. (2006). Evaluating crop models. In D. Wallach, D. Makowski, & W. J. James (Eds.). *Working with Dynamic Crop Models Evaluation, Analysis, Parameterization, and Applications* (First edition ed., pp. 11-51). Amsterdam, Netherlands: Elsevier.
- Wang, F., Pei, M., Qiu, L., Yao, Y., Zhang, C., & Qiang, H. (2019). Performance of anaerobic digestion of chicken manure under gradually elevated organic loading rates. *International Journal of Environmental Research and Public Health* 16(12). doi: [10.3390/ijerph16122239](https://doi.org/10.3390/ijerph16122239)
- Wang, J., Liu, B., Sun, M., Chen, F., Terashima, M., & Yasui, H. (2022). A kinetic model for anaerobic digestion and biogas production of plant biomass under high salinity. *International Journal of Environmental Research and Public Health* 19(11). doi: [10.3390/ijerph19116943](https://doi.org/10.3390/ijerph19116943)
- Wichern, M., Gehring, T., Fischer, K., Andrade, D., Lübken, M., Koch, K., . . . Horn, H. (2009). Monofermentation of grass silage under mesophilic conditions: Measurements and mathematical modeling with ADM 1. *Bioresource Technology* 100(4), 1675-1681. doi: [10.1016/j.biortech.2008.09.030](https://doi.org/10.1016/j.biortech.2008.09.030)